

PAPER

Design, simulation and testing of a novel radial multi-pole multi-layer magnetorheological brake

To cite this article: Jie Wu *et al* 2018 *Smart Mater. Struct.* **27** 025016

View the [article online](#) for updates and enhancements.

Design, simulation and testing of a novel radial multi-pole multi-layer magnetorheological brake

Jie Wu^{1,2}, Hua Li², Xuezheng Jiang² and Jin Yao²

¹ School of Mechanical Engineering, Xihua University, Chengdu 610039, People's Republic of China

² School of Manufacturing Science and Engineering, Sichuan University, Chengdu 610065, People's Republic of China

E-mail: sculihua2005@sina.com

Received 23 November 2017

Accepted for publication 5 January 2018

Published 24 January 2018



Abstract

This paper deals with design, simulation and experimental testing of a novel radial multi-pole multi-layer magnetorheological (MR) brake. This MR brake has an innovative structural design with superposition principle of two magnetic fields generated by the inner coils and the outer coils. The MR brake has several media layers of magnetorheological (MR) fluid located between the inner coils and the outer coils, and it can provide higher torque and higher torque density than conventional single-disk or multi-disk or multi-pole single-layer MR brakes can. In this paper, a brief introduction to the structure of the proposed MR brake was given first. Then, theoretical analysis of the magnetic circuit and the braking torque was conducted. In addition, a 3D electromagnetic model of the MR brake was developed to simulate and examine the magnetic flux intensity and corresponding braking torque. A prototype of the brake was fabricated and several tests were carried out to validate its torque capacity. The results show that the proposed MR brake can produce a maximum braking torque of 133 N m and achieve a high torque density of 25.0 kN m^{-2} , a high torque range of 42 and a high torque-to-power ratio of 0.95 N m W^{-1} .

Keywords: magnetorheological (MR) brake, multi-pole, multi-layer, braking torque, torque density

(Some figures may appear in colour only in the online journal)

1. Introduction

Magnetorheological (MR) fluid is a typical smart material which is mainly composed of micrometer-sized ferromagnetic particles, the carrier fluid and the additives [1]. When subjected to a magnetic field, the fluid translates from Newtonian fluid into Bingham fluid quickly and reversibly, and it develops a yield stress due to that the particles are gathered to form chain-like structures in the direction of the magnetic flux. The yield stress is strongly dependent on the applied magnetic field [2]. Due to its controllable and rapid variable viscosity, it can be widely used in the design of mechanical torque transmission devices, such as dampers [3–5], brakes [6–10], clutches [11–13], shock absorbers [14], engine mounts [15, 16] and robotics [17].

In recent years, MR brakes have received considerable attention. Researchers have developed various MR brakes with different structures, and their attention is not only on the maximum braking torque but also on the torque density which is defined by the ratio of maximum braking torque divided by the overall dimensional volume of the brake. Generally, MR brakes commonly can be divided into two categories according to their working surface: disc type and cylindrical type.

For a disc type, the MR fluid is placed in a small gap which is perpendicular to the rotation axis. The Lord Corporation developed a rotary MRB-2107-3 MR brake [18], the maximum output is nearly 5.6 N m. Zhou *et al* [19] studied a compact double-disk MR fluid brake with two shear discs and a coil, the maximum transmitted torque is 3.5 N m. Sarkar

et al [20] developed a disc-type MR brake that operating under compression plus shear mode of MR fluid, increasing the maximum torque to nearly 100 N m. Song *et al* [10] proposed a disc-type MR brake adjustable gap. Kikuchi *et al* [21] studied a multilayered MR brake. For a cylindrical type, the MR fluid is working in an annular gap which is parallel to the rotation direction. Senkal *et al* [22] designed a MR brake with serpentine flux path, the maximum transmitted torque is 10.9 N m. Rossa *et al* [23] developed a multilayered wide-ranged torque MR brake with four annular fluid gaps, and the brake has a torque to volume ratio of 48.1 kN m^{-2} and a maximum-to-minimum torque ratio of 176. Rossa *et al* [24] also discussed the torque density, efficiency, bandwidth and controllability of different MR brakes, including a single disc brake, a single drum brake, multiple-disc based brakes and multiple-cylinder based brakes. So far, there are also several innovative MR brake designs with improved torque performance have been proposed.

There are few researches on maximizing the torque in a given volume by increasing the number of annular working gaps. Shiao *et al* [25] presented a multi-pole MR brake. This brake is working in cylindrical type and is set up several coils along the circumferential direction ensuring that the entire MR fluid in the cylinder gap can be activated. The ratio of the torque to volume of this brake is only about 13 kN m^{-2} . Lately, Shiao *et al* [7] also presented a multipole bilayer magnetorheological brake and the torque density is 25.8 kN m^{-2} , but the maximum braking torque is only 27.5 N m.

To develop a high torque density MR brake, a high torque-to-power ratio with a large torque range, a novel radial multi-pole multi-layer MR brake was designed in the current study, and a comprehensive analysis involving working principle, braking torque analysis, magnetostatic simulation, and experimental tests was conducted. This MR brake has six inner electromagnetic poles, six outer electromagnetic poles and four MR fluid layers. In this paper, the design of the proposed MR brake is firstly described in detail. The design considerations include the form of the transmission, the braking torque and the magnetic circuit. Then, to investigate the magnetic effect on the MR brake, a magnetostatic simulation was conducted to validate the designed magnetic circuit. Finally, a prototype was fabricated and assembled, and some tests were conducted to validate the proposed MR brake. Experimental results concerning the torque range, the transmission torque per power and the torque density. In addition, the test results were compared with those of conventional MR brakes.

2. Design of RMPML MR brake

2.1. Operating concept

The drum-shaped MR brake operates in the shear mode. In this work, a new radial multi-pole multi-layer (RMPML) MR brake shown in figure 1 was proposed to increase the torque density in a given volume. The proposed MR brake is

implemented by two sets of coils: inner coils and outer coils, and the magnetic circuit is shown in figure 2. As can be seen, each layer can transmit torque separately. As shown in figure 1(a), it contains an inner stator with six electromagnetic poles with winding coils, an outer stator with six electromagnetic poles with winding coils, three cylinders (cylinder A, cylinder B and cylinder C), and four MR fluid layers located between the upper part of the inner stator and the lower part of the outer stator. The cylinder A and cylinder C are connected to the rotary shaft, while the cylinder B is connected to the stationary housing. And the inner stator and the outer stator are also connected to the stationary housing. As shown in figure 1(b), two adjacent electromagnetic poles of the inner stator are connected by aluminum plate in order to make the produced magnetic flux penetrates MR fluid working gaps, and similar to the two adjacent electromagnetic poles of the outer stator. The direction of magnetic flux in each pole of the inner stator is opposite to that of its two adjacent poles, while the direction of magnetic flux in each pole of the outer stator is opposite to that of its two adjacent poles. Besides, the direction of magnetic flux in the pole of the inner stator is the same as that of the pole of the outer stator when the two poles are in the same radial direction. The MR fluid contained in the four working gap is subject to shear due to slippage between the cylinder A and cylinder B, cylinder C and cylinder B.

As shown in figure 2, the magnetic flux travels following the path of the black lines and arrows when all coils are energized, and it will travel from one pole of the inner stator, through four MR fluid working gaps and three cylinders, into the pole of the outer stator, back to the four MR fluid working gaps and three cylinders, and finally back to the pole of the inner stator.

In this proposed design, the effect of centrifugal force on transmission torque is expected to be smaller than that of disc structures because of the shorter radial critical area in the former, which allows free outward movement of the particles. It ensures that almost the entire MR fluid in four annular MR fluid working gaps has been activated when applying a current to the coils. The MR fluid becomes magnetically permeable after applying a current to all coils, and the chain of MR particles forms a route for magnetic flux to pass through. Thus, the permeable MR fluid within the four working gaps functions as a resistance for the MR brake. Consequently, the RMPML MR brake provides a more effective torque enhancement because of the design of the two sets of coils and the four annular fluid working gaps. The number of the poles is depended on the size of the brake and manufacture abilities, such as four, six, eight, ten stators and so on. In this paper, the performance of a twelve poles' MR brake has been studied. The major design parameters are also defined as shown in figure 3.

Sealing of the MR brake is another important design criterion. The risk of sealing failure is increased due to that the iron particles in the MR fluid. In this RMPML MR brake, two Rectangle Co-axial seals employed between the rotating shaft and the stationary housing were used to seal the MR

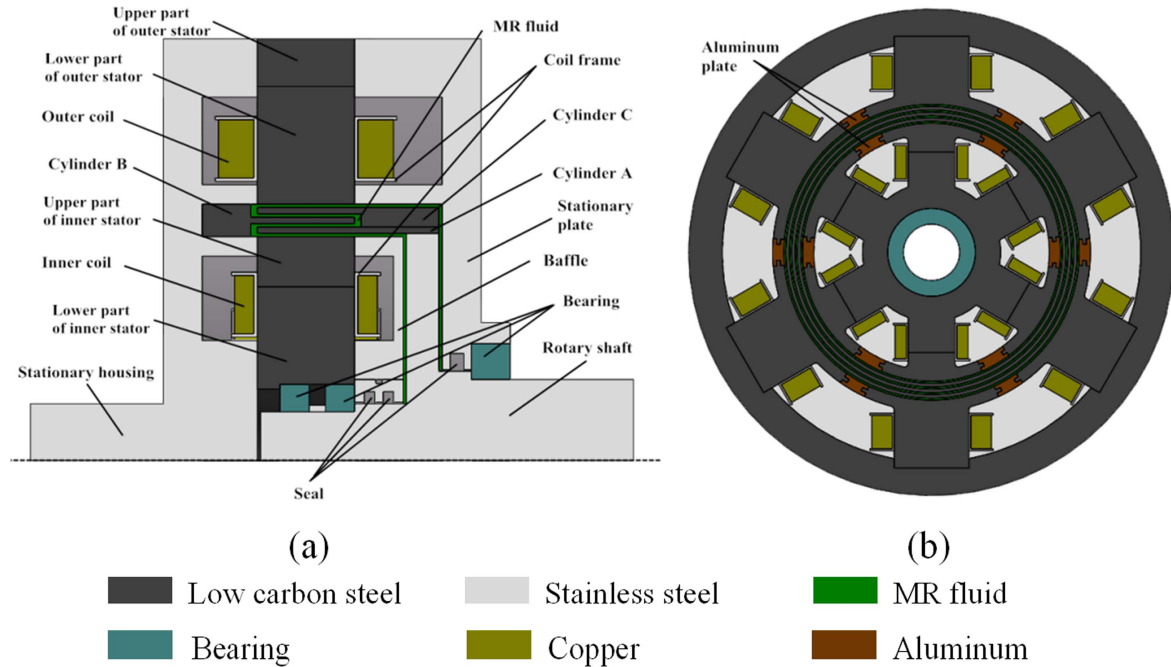


Figure 1. Radial multi-pole multi-layer MR brake: (a) schematic diagram of RMPML MR brake; (b) the crosssectional view showing a configuration of the four gaps is between the inner stator and the outer stator.

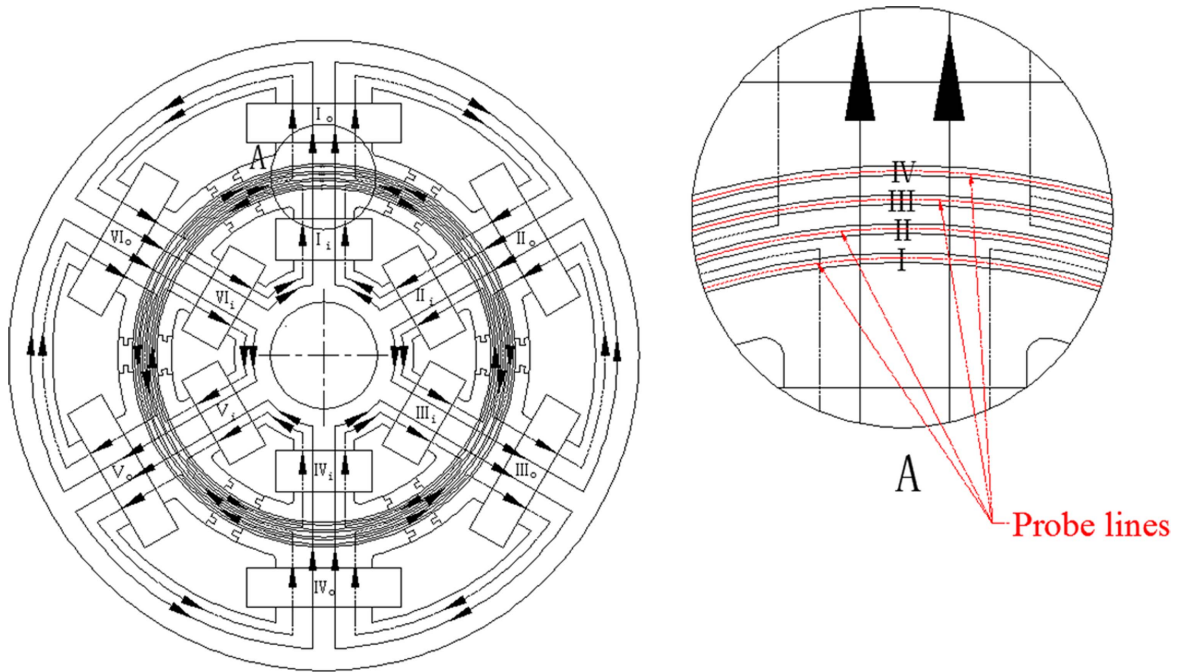


Figure 2. Sketch of the designed magnetic circuit.

fluid in the gap, and Viton O-rings were used for the static applications.

2.2. The analysis of braking torque

The MR fluid is an essential of the RMPML MR brake, and its viscosity without a magnetic field and shear stress gradient with respect to the applied magnetic field strength are the standard of material selection. Lord MRF-132DG, as seen in

table 1 (data was referred from Lord technical papers [26, 27]), was selected in this MR brake because of its higher yield stress than that of other MR fluids.

It is well known that MR fluid behaves in the liquid state like Bingham plastics

$$\tau = \tau_y(B) + \eta\dot{\gamma}, \quad (1)$$

where τ is the total shear stress, τ_y is the yield stress caused by the applied magnetic field, B is the radial component of

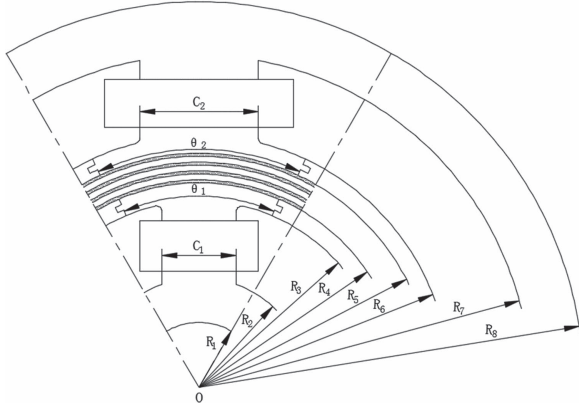


Figure 3. Definitions of design parameters.

Table 1. Properties of Lord MRF-132DG MR fluid.

Property	Value
Carrier liquid	Hydrocarbon
Yield strength (kPa) at 100 kA m ⁻¹	23
Yield strength (kPa) at 200 kA m ⁻¹	42
Plastic viscosity (Pa s) at 40 °C	0.112
Density (g cm ⁻³)	3.09
Operating temperature (°C)	-40 to +130
Thermal conductivity (W m ⁻¹ °C ⁻¹) at 25 °C	0.25–1.06

magnetic flux density (that is the component orthogonal to the transmission surfaces) in this cylindrical MR brake, η is the viscosity of the MR fluid with no applied magnetic field, and $\dot{\gamma}$ is the shear rate of the MR brake in the shear mode.

$$\dot{\gamma} = \frac{R\omega}{h}, \quad (2)$$

where R is the relevant radius of the gap, ω is the angular velocity of the shaft and h is the thickness of the MR fluid gap.

From the experimental results of the yield stress of liquid MRF-132DG, the relationship between yield stress $\tau_y(B)$ (kPa) and magnetic flux density B (T) is established by using a least square curve fitting method [26]

$$\begin{aligned} \tau_y(B) = & 52.962B^4 - 176.51B^3 + 158.79B^2 \\ & + 13.708B + 0.1442. \end{aligned} \quad (3)$$

Regardless of the given geometry, the tangential resistive force is calculated by integrating τ over the shearing surfaces. For the rotary MR brake in this paper, taking into the radius R_{MR} between this surface and the rotation axis, the braking torque generated by one MRF layer can be determined as follows

$$T_{MR} = R_{MR} \int_0^z \int_0^{2\pi} R_{MR} \tau_y d\theta dz + \frac{2\pi\eta\omega}{h} R_{MR}^3 z, \quad (4)$$

where z is the axial width of one MRF layer.

The braking torque for four MR fluid working gaps is given by the sum of the torque delivered by each MR fluid surface. Finally, the total braking torque produced by the MR

brake is

$$\begin{aligned} T = & T_{MR1} + T_{MR2} + T_{MR3} + T_{MR4} + T_{non} + T_{fr} \\ = & \left(R_{MR1} \int_0^z \int_0^{2\pi} R_{MR1} \tau_y d\theta dz \right. \\ & + R_{MR2} \int_0^z \int_0^{2\pi} R_{MR2} \tau_y d\theta dz \\ & + R_{MR3} \int_0^z \int_0^{2\pi} R_{MR3} \tau_y d\theta dz \\ & \left. + R_{MR4} \int_0^z \int_0^{2\pi} R_{MR4} \tau_y d\theta dz \right) \\ & + \left[\frac{2\pi\eta\omega z}{h} (R_{MR1}^3 + R_{MR2}^3 + R_{MR3}^3 + R_{MR4}^3) + T_{non} \right] \\ & + T_{fr}, \end{aligned} \quad (5)$$

where R_{MR1} , R_{MR2} , R_{MR3} and R_{MR4} are the radius of the four MR fluid working gaps, respectively. T_{non} is the viscous torque of non-working areas of the MR fluid which depends on the rotational velocity ω . T_{fr} is the friction torque resulting from the bearing and sealing parts in the MR brake.

It is obviously seen that the total braking torque is mainly composed of three components: the field torque, the viscous torque (working and non-working areas) and the friction torque. The controllable field torque which is affected by the yield stress of MR fluid and the locations of MR fluid gaps is the major component of the total torque. The torque enhancement can be achieved by increasing the magnetic field strength within the MR fluid. This is the advantage of the RMPML MR brake.

3. Magnetostatic simulation of the circuit

In this section, the magnetostatic simulation of the circuit was carried out to validate the designed magnetic circuit and analyze the magnetic induction of the four working gaps. The simulation could be considered as a 3D problem due to the design of several coils. Table 2 lists the parameters of the fluid, the ferromagnetic path and the coil adopted in the simulations. For the magnetostatic simulation, the MR fluid and the low-carbon steel are nonlinear ferromagnetic materials, whose material properties are defined by the B - H curves [27, 28], while the relative permeability of the non-ferromagnetic materials, including stainless steel, aluminum and air, was set to 1. The current in each coil was applied on the coil cross-section as coil turns and coil current. The standard wire gauge (Polyester Enamelled Round Copper Wire, QZ-1, $\Phi = 0.72$ mm) which has been considered for the simulation has been added in table 2.

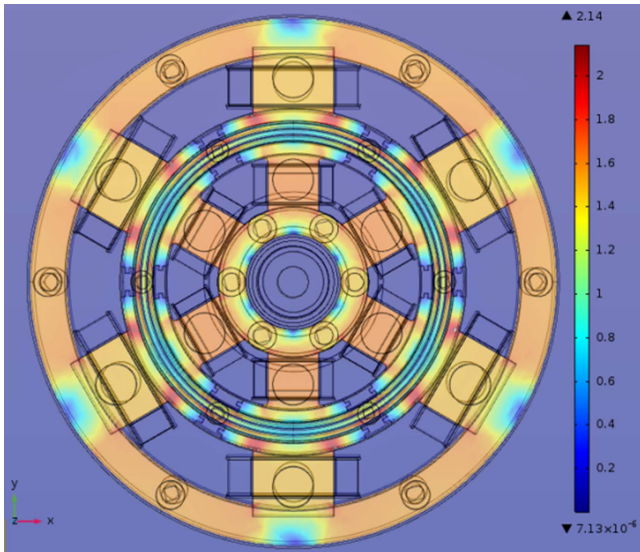
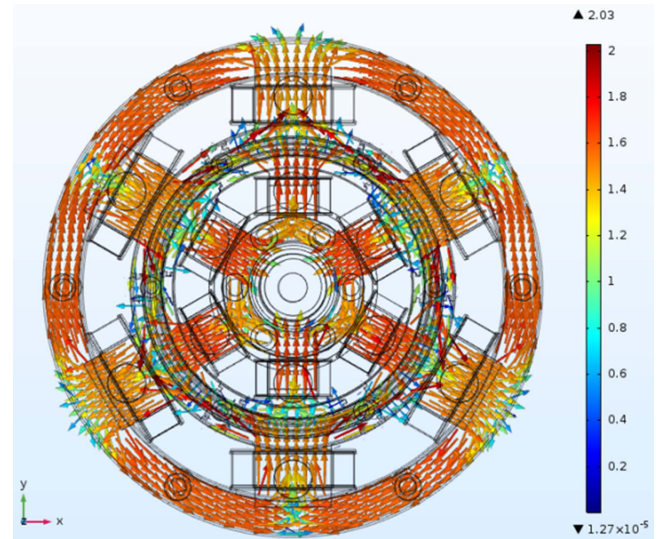
3.1. Magnetic field distribution

Figure 4 shows the direction of the magnetic flux in the cross-section of the MR brake when applying a 2 A input current to each coil. It can be observed that it has a maximum value of nearly 2.14 T at the areas of outer stator, which are located near the corner of the lower part of the outer stator.

Figure 5 presents the flow direction of the magnetic flux in the cross-section of the RMPML MR brake. It can be seen that most of the magnetic flux orthogonally penetrates the MR

Table 2. Invariant parameters in the analytical model.

Parameter	Term	Value	Unit
Inner stator width	C_1	25	mm
Outer stator width	C_2	40	mm
Inner stator angle	θ_1	46	degree
Outer stator angle	θ_2	50	degree
Inner stator radii	R_1, R_2, R_3, R_4	23.5, 37, 63, 69	mm
Outer stator radii	R_5, R_6, R_7, R_8	79, 85, 112, 130	mm
MR fluid axial width	z	30	mm
Inner coil input power	$N_i I_i$	400	Ampere-turns
Outer coil input power	$N_o I_o$	700	Ampere-turns
Coil diameter	Φ	0.72	mm

**Figure 4.** Magnetic flux density distribution in the cross-section of the RMPML MR brake.**Figure 5.** Flow direction of the magnetic flux in the RMPML MR brake.

fluid in the four working gaps, so magnetic particles in the MR fluid form up to become many chains. As a result, the braking torque is produced a resistance to the relative rotation. The braking torque can be easily controlled by the magnitudes of the input current. The result confirms the feasibility of the operating concept and magnetic circuit design of the RMPML MR brake.

3.2. Magnetic flux density of the working gaps

Figure 6 is the magnetic flux density on the four cylindrical surfaces: (a) MR fluid gap I; (b) MR fluid gap II; (c) MR fluid gap III; (d) MR fluid gap IV. For the cylindrical areas of MR fluid gap I and MR fluid gap IV, the red pattern is interspersed by dark-blue areas, which are the areas between two adjacent inner stators or two adjacent outer stators. In these areas, the magnetic flux density was lower due to the aluminum plates. In addition, the high magnetic flux density is observed in areas near inner stator and outer stator. Along the MR fluid cylindrical surfaces, the magnetic flux density is apparently non-uniform, and the low flux density is about zero while the maximum flux density is more than 1.0 T. Due to the varied

magnetic flux density, the generated yield stress is also non-uniform. For the design of several inner stators and outer stators, the magnetic flux was employed effectively to increase the magnetic field strength within the MR fluid, especially in the areas of inner stators and outer stators. The magnetic field strength can be adjusted by the configuration of several inner and outer stators as well as the input current. Most of the flux after flowing through the four MR fluid gaps and three cylinders will go to the inner stator and outer stator.

In addition, the magnetic flux density on the cylindrical surfaces along the axial direction apparently remains unchanged, so it is feasible to achieve the torque enhancement by increasing the axial length of MR fluid surfaces. In summary, torque enhancement can be achieved by increasing the axial or the radial dimensions of the MR fluid gaps.

The generated torque of the RMPML MR brake depends on the magnitude of magnetic flux density in four MR fluid gaps. To investigate it, four probe lines were drawn along the circumference and in the middle of these gaps (gap I, gap II, gap III and gap IV). Figure 7 shows the magnetic flux density along four probe lines: (a) MR fluid gap I; (b) MR fluid gap II; (c) MR fluid gap III; (d) MR fluid gap IV, while the input

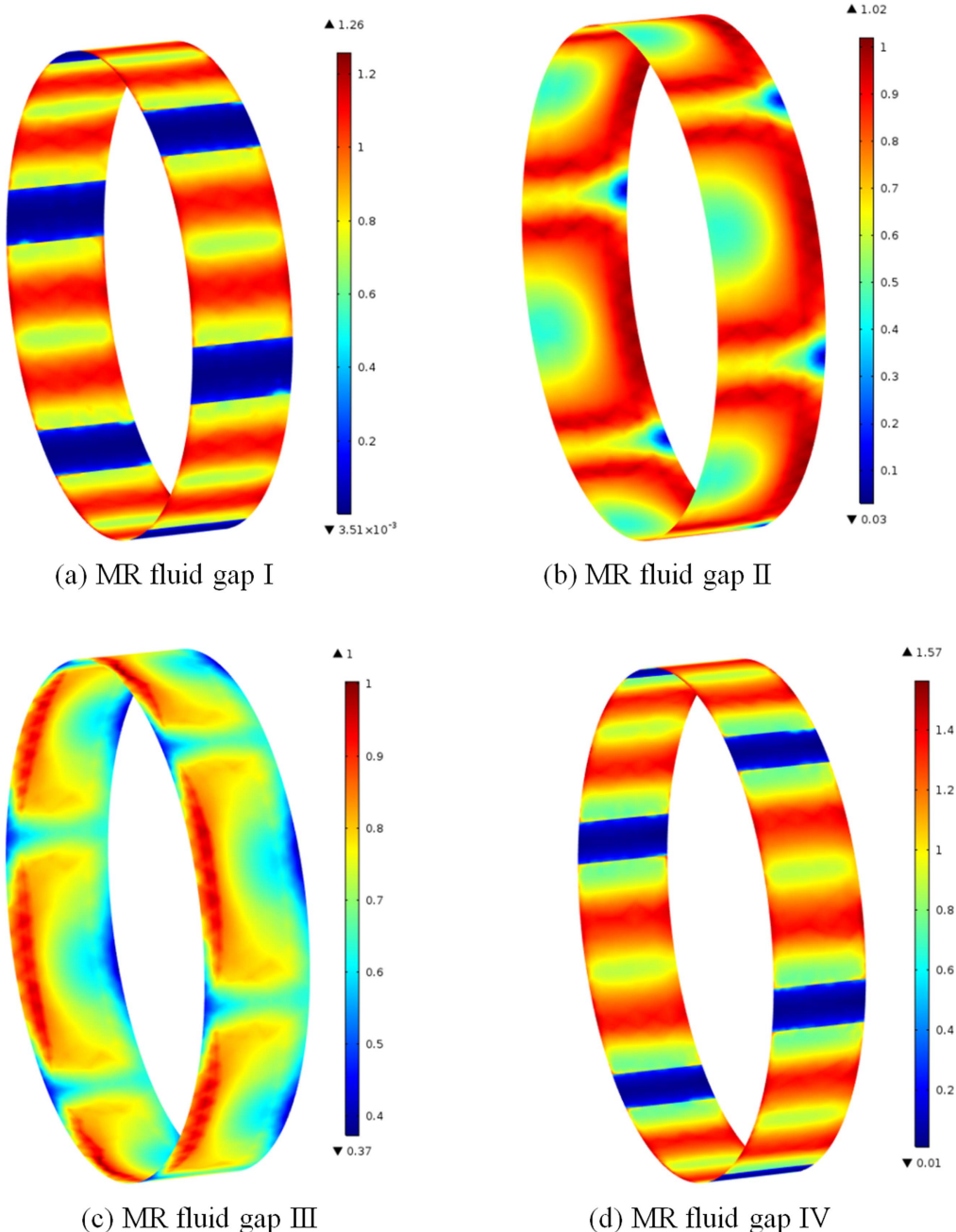


Figure 6. Magnetic flux density within the four gaps along the axial direction.

current I changes from 0.5 to 2.0 A. It can be seen that almost all the MR fluid in the working gaps has been activated. The positions of six inner stators (or six outer stators) are indicated by the six peaks in the figures 7(a)–(d). In the space between two adjacent inner or outer stators, the flux density is nearly zero, which means the aluminum plates have almost isolated the flux from going directly from one inner stator (or outer stator) to the adjacent inner stators (or outer stators) rather than through the MR fluid gaps. The magnetic flux density in the MR fluid gap II and gap III is smaller than that in the MR fluid gap I and gap IV while the input current is fixed. This is due to some magnetic flux travels directly from the circumferential direction of each cylinder rather than through the MR fluid gaps. The magnetic flux density of the MR fluid in

the four gaps and the generated torque can meet the design requirements. This further illustrates that the magnetic circuit of the designed MR brake is feasible and efficient.

Figure 8(a) shows the magnetic flux density distribution when only six inner coils are energized, and the magnetic flux density distribution when only six outer coils are energized is shown in figure 8(b). Because the winding coils for two adjacent poles are wound in opposite directions, the magnetic field flux travels from one pole to its two adjacent poles. If only six inner coils are energized, the most magnetic flux runs between two adjacent inner stators. And when only six outer coils are energized, the most magnetic flux runs between two adjacent outer stators. As mentioned above, not all the MR fluid in the working gaps can be activated, thus the generated

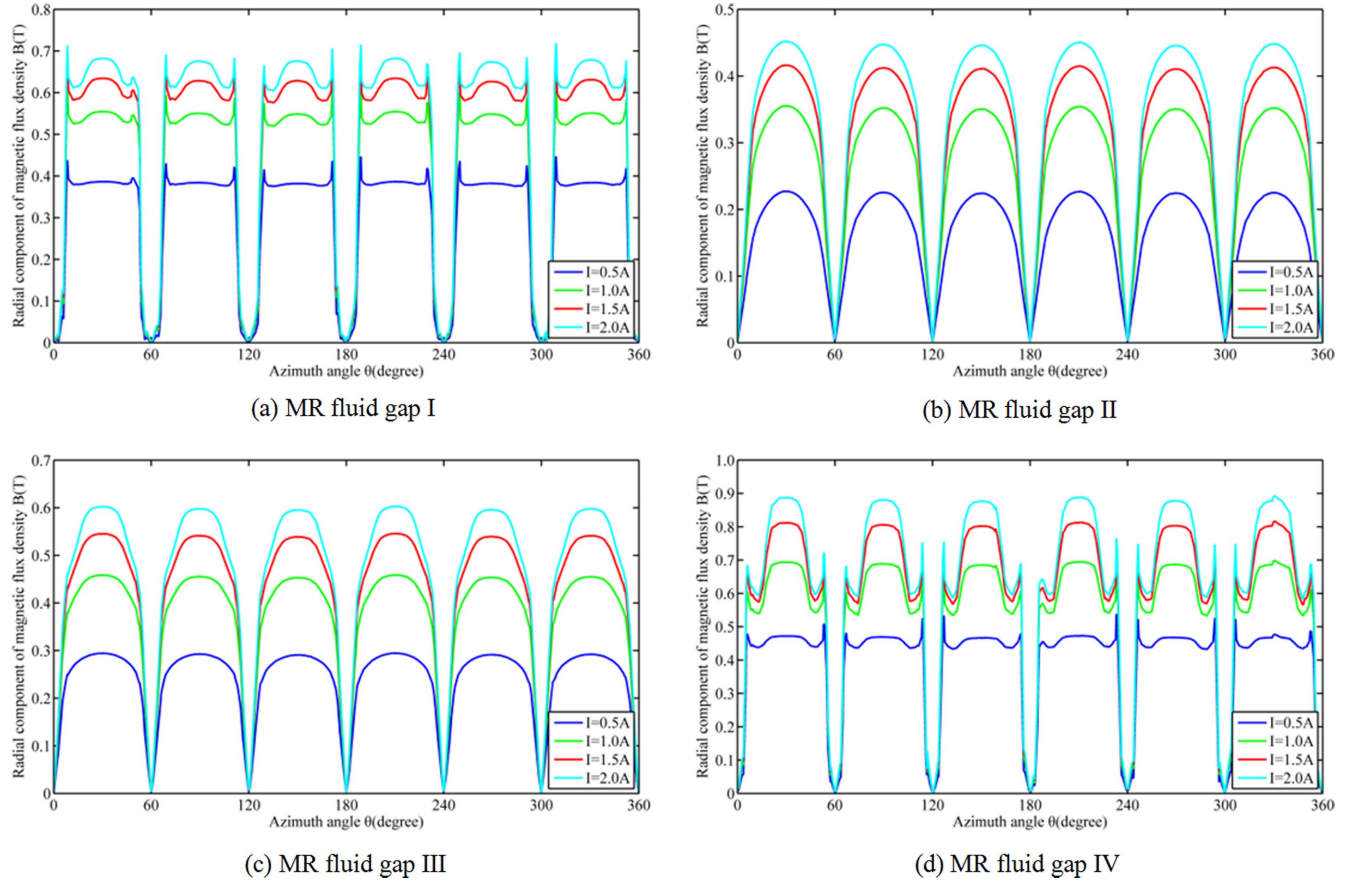


Figure 7. Radial component of magnetic flux density distribution along the middle line of: (a) MR fluid gap I; (b) MR fluid gap II; (c) MR fluid gap III; (d) MR fluid gap IV.

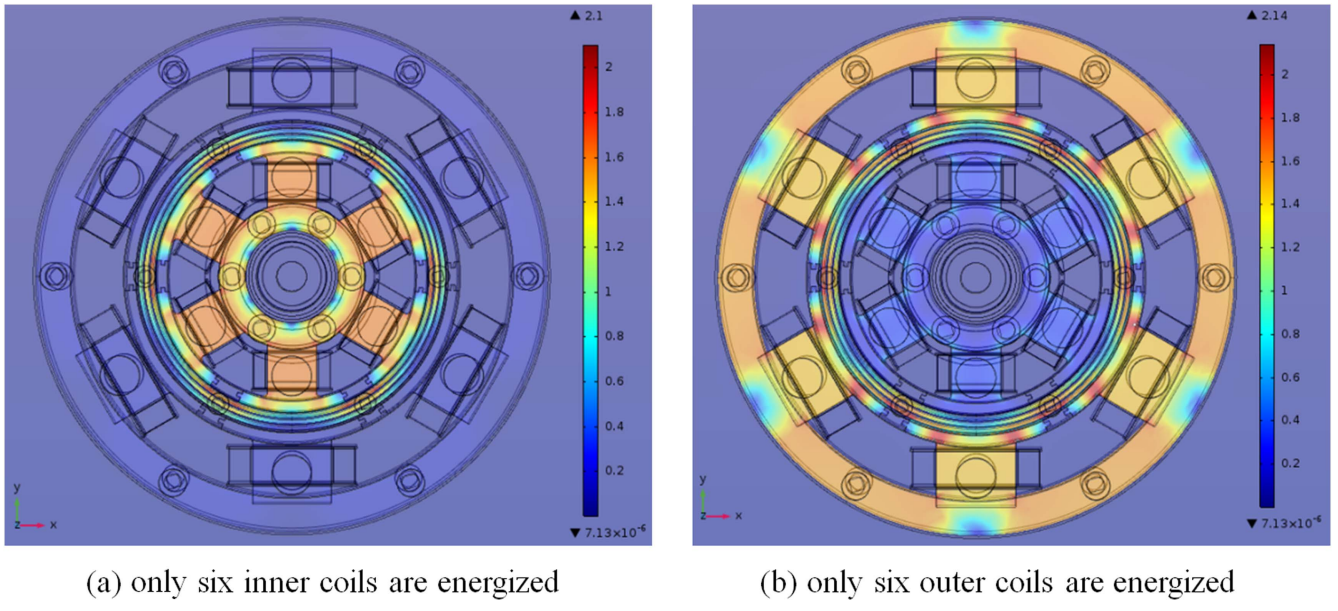


Figure 8. Magnetic flux density distribution of cross section of RMPML MR brake.

torque will be smaller than that when all the inner coils and outer coils are energized.

Details of the magnetic flux density in the cross-section of the same direction of current applied in both the coils and opposite direction of current applied in the both the coils are

shown in figure 9. When the direction of the current applied in the inner stator is the same as that in the outer stator and the two poles are in the same radial direction, the low-carbon steel becomes saturated at around 2.14 T, as shown in figure 9(a). It indicates that the magnetic flux travels

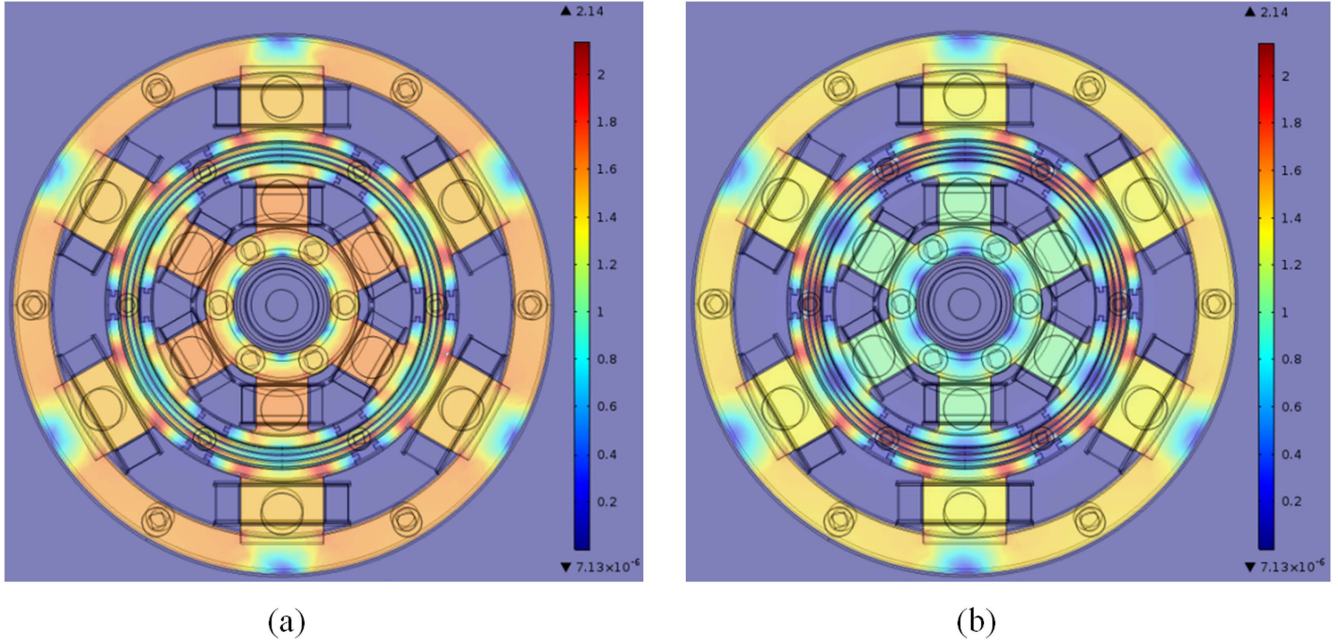


Figure 9. Magnetic flux density distribution of cross section of RMPML MR brake: (a) the direction of the current applied in the inner stator is the same as that in the outer stator when the two poles are in the same radial direction; (b) the direction of the current applied in the inner stator is opposite to that in the outer stator when the two poles are in the same radial direction.

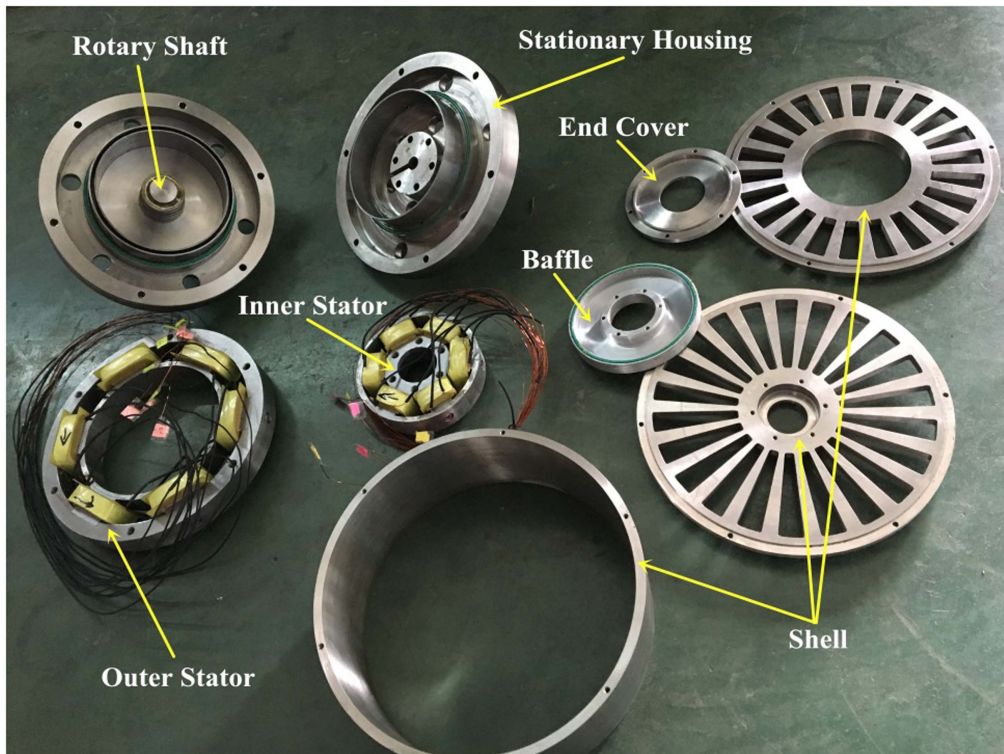
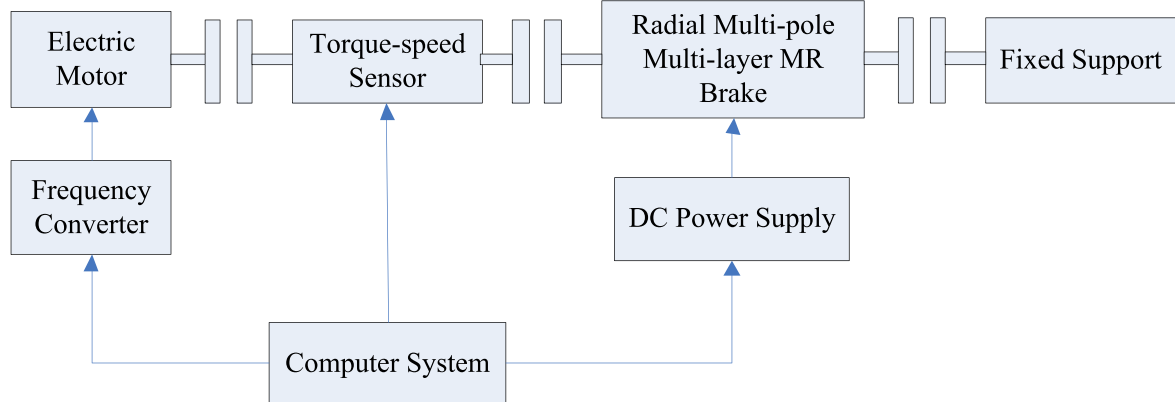
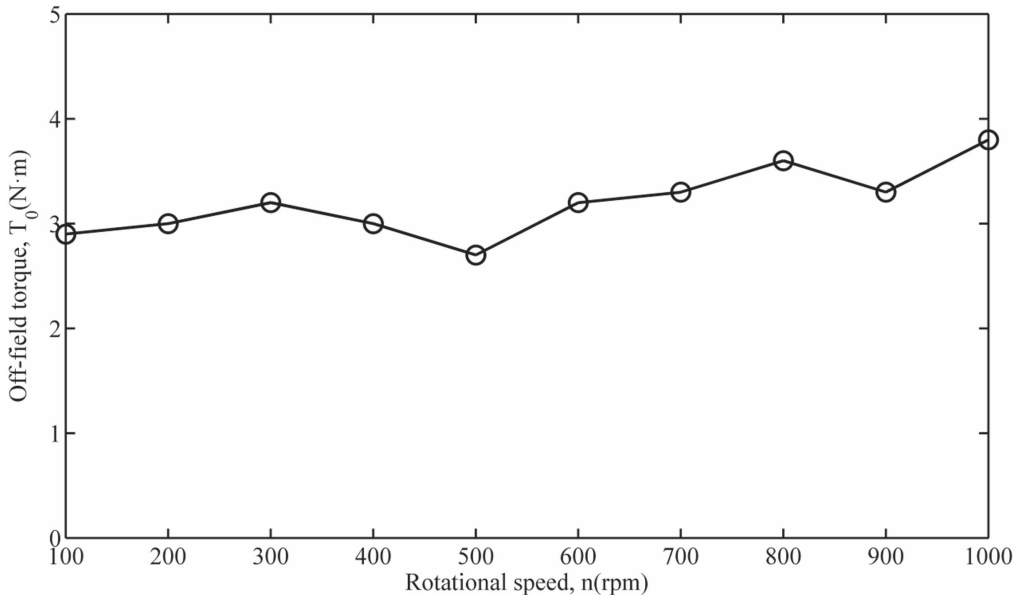


Figure 10. Main components of proposed RMPML MR brake prototype.

following the path of the black lines and arrows as shown in figure 2, and almost all the MR fluid within four gaps has been activated. The magnetic flux density can be increased with superposition principle of two magnetic fields generated by the inner coils and the outer coils. Figure 9(b) shows the magnetic flux density of cross section of the proposed brake

when the direction of the current applied in the inner stator is opposite to that in the outer stator and the two poles are in the same radial direction. From the figure, it can be seen that the magnetic flux density is lower than 1.0 T and the magnetic flux density within four fluid gaps is also much lower than that in figure 9(a). This is due to that the trends of the

**Figure 11.** Experiment layout of proposed RMPML MR brake.**Figure 12.** Off-field torque at various rotational speeds.

magnetic field lines of the inner coil and the outer coil in the same radial direction are deviating from each other, and the magnetic field at a certain point is the vector sum of the magnetic fields generated by the different magnetic field sources.

4. Experimental evaluation of the prototype

4.1. Prototype of proposed MR brake and experimental setup

Figure 10 shows the main components of proposed RMPML MR brake prototype. Copper wires with a diameter of 0.72 mm are used for both the inner coil and outer coil. The maximum input current of the wire is 2 A, and each inner coil with 200 turns of winding and each outer coil with 350 turns of winding are able to provide a sufficient magnetic field for the working gaps. Baffle was used to protect the coils from inward MR fluid, and end cover was used to hold the bearing.

Figure 11 shows the experiment layout of the proposed RMPML MR brake. It mainly consists of electric motor,

torque sensor, fixed support, power supply, computer system and the proposed MR brake. The MR brake is connected to a torque sensor and driven by an electric motor, and the output of the MR brake is fixed by a fixed support. The computer system is used to acquire the signal from the torque sensor, and the measurement range of the torque of the torque sensor can be extended to 200 N m. Power supply is used as a current amplifier to supply the exact current to the brake.

4.2. Torque analysis in the RMPML MR brake

To evaluate the proposed RMPML MR brake, the off-field torque and the maximum generated torque were performed. The off-field torque generated by the mechanical friction and the fluid viscosity is initially measured. In the experiment, the rotational speed is regulated to be various values by the inverter. Figure 12 shows the Off-field torque at various rotational speeds. From the figure, the off-field torque rises slightly as the rotational speed increases, and the value is around 3.2 N m. This is mainly due to that the viscous torque

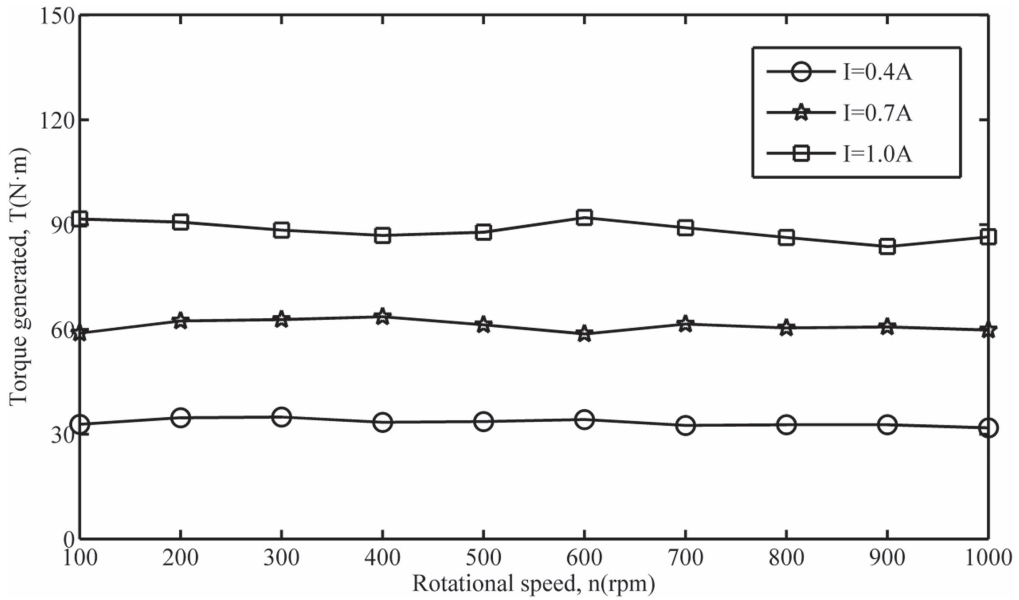


Figure 13. Total generated torque versus rotational speed at different input currents.

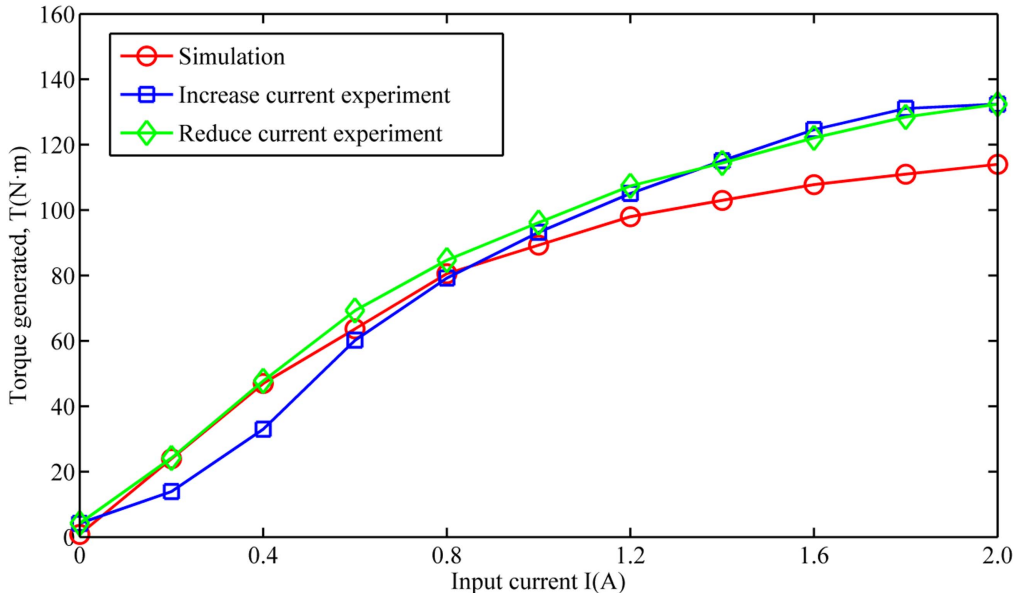


Figure 14. Braking torque of proposed RMPML MR brake.

and the friction torque increase as the rotational speed increases.

Figure 13 shows the total generated torque versus rotational speed at different input currents. The input currents are 0.4, 0.7 and 1.0 A, respectively. It can be observed from the figure that the effect of rotational speed is minimal on the total generated torque. The proposed MR brake performs torque-constant characteristic, and the generated torque is mainly related to the input current and the speed. Therefore, the developed MR brake can be controlled easily.

The input current was set in the range of 0–2.0 A and the rotational speed was set at 200 rpm to obtain the braking torque of the RMPML MR brake. Figure 14 shows the details of the torque results at different input currents from simulation and experiment. The generated torque level can be

accurately controlled by the input current. As the input current continues to increase, the increasing trend of braking torque gradually slows down until it reaches a steady value. This phenomenon is caused by the magnetic saturation of MR fluid. As this figure illustrates, the maximum braking torque is 133 N m according to the experimental results. The maximum simulated torque generated by the MR brake is nearly 120 N m. It is observed that the maximum experimental torque is 133 N m while the maximum simulated torque is 117 N m, all at 2.0 A input current. The difference between experimental and simulated torque can be attributed to the viscosity torque and the friction torque, which is negligible in the simulation model. In addition, the manufacture and assembly of the prototype is also a factor. It also can be seen that the two curves basically coincide when gradually

Table 3. Specifications of the proposed brake and comparison to other documented results.

	Designed MR brake	Lord RD- 2078-1	Single- plate MR brake	Serpentine MR brake	Multi-pole MR brake	Multi- layered MR brake	Multi-pole bilayer MR brake
Maximum torque (N m)	133	4.0	7	10.9	19.9	5.3	27.5
Off-state (N m)	3.2	0.4	0.5	0.1	—	0.03	2
Length (mm)	98	35.7	21	89.7	98	39	136
Radius (mm)	130	96.6	78	31.75	70	30	50
Power (W)	140	15	—	20	15.3	19	38.1
Torque/volume (kN m/m ³)	25.0	12.5	17.4	38.3	13.1	48.1	25.8
Torque/power (N m/W)	0.95	0.26	—	0.54	1.30	0.28	0.72
Controllability	42	10	14	109	—	176	14

increasing the input current and decreasing the input current. This phenomenon indicates that the proposed MR brake has good magnetic characteristics.

This paper is to improve the torque density of the MR brake devices by using a novel radial multi-pole multi-layer configuration. The considered evaluation criteria are the torque density, the controllability and the torque per power. Torque density which is defined by the ratio of maximum generated torque divided by the geometric volume of the MR brake, controllability is defined by the maximum to minimum torque ratio, and torque per power ratio which is defined by the ratio of maximum generated torque divided by the power consumption, have been investigated. Then, a comparison of the designed MR brake proposed in this paper with other typical MR brakes (Lord RD-2087-01 [18], single-plate MR brake [29], serpentine MR brake [22], multi-pole MR brake [25], multi-layered MR brake [23], multi-pole bilayer MR brake [7]) presented in the state of art is necessary. Table 3 compares the design specifications of the proposed brake to a commercially available brake and some brakes available in the literature. When exploited up to its complete saturation, the brake can generate 133 N m. This gives a torque density of 25.0 kN m⁻², a maximum-to-minimum torque ratio, taking into consideration the Coulomb friction, of 42 and a torque-to-power of 0.95 N m W⁻¹. The designed brake provides two times torque density, four times maximum-to-minimum torque ratio and about four times torque-to-power ratio, compared to the commercial brake. The high controllability, high torque-to-power ratio and high torque density make the actuator amply adaptable for various applications.

Compared to the conventional MR brakes, the radial multi-pole multi-layer MR brake looks complicated and has high manufacturing cost compared with single-disk MR brakes. Future work should focus on the dynamic response analysis, control, thermal characteristics, cooling management and structural improvement of the manufactured prototype.

5. Conclusions

This paper presented systematic investigations, including innovative designing, theoretical analysis on output torque and simulation evaluating of a novel radial multi-pole multi-layer MR brake. The main conclusions are obtained as follows:

- (a) An innovative MR brake with superposition principle of two magnetic fields generated by the inner coils and the outer coils was designed and manufactured.
- (b) Torque enhancement of the proposed MR brake can be achieved by increasing the axial or the radial dimensions of MR fluid gaps from simulation results.
- (c) From the experimental results, the two curves of the measured torque basically coincide when gradually increasing and decreasing the input current. It indicates that the proposed MR brake has good magnetic characteristics.
- (d) The proposed radial multi-pole multi-layer MR brake has higher torque density, higher controllability and higher torque-to-power ratio based on the experimental results. It is promising for applications in many situations of high braking torque and compact design.

Acknowledgments

This work was supported by the Applied Basic Research Programs of Sichuan Province (Grant No. 2012JY0085). This work was also supported by the National Key Research and Development Plan (2016YFD0700400), Research Project of Key Laboratory Machinery and Power Machinery (Xihua University), Ministry of Education (JYBFX-YQ-1), and Sichuan Provincial Department of Science and Technology Projects (2017TD0023).

ORCID iDs

Hua Li  <https://orcid.org/0000-0002-5748-2376>

References

- [1] Lucking Bigu J, Charron F O and Plante J B 2015 Understanding the super-strong behavior of magnetorheological fluid in simultaneous squeeze-shear with the Péclet number *J. Intell. Mater. Syst. Struct.* **26** 1844–55
- [2] Kumbhar B K, Patil S R and Sawant S M 2015 Synthesis and characterization of magneto-rheological (MR) fluids for MR brake application *Eng. Sci. Technol. Int. J.* **18** 432–8

- [3] Kim W H *et al* 2017 A novel type of tunable magnetorheological dampers operated by permanent magnets *Sensors Actuators A* **255** 104–17
- [4] Hu G *et al* 2017 Development of a self-sensing magnetorheological damper with magnets in-line coil mechanism *Sensors Actuators A* **255** 71–8
- [5] Park J, Kang J and Choi S 2016 Design and analysis of above knee prosthetic leg using MR damper *Trans. Korean Soc. Noise Vib. Eng.* **26** 165–71
- [6] Wu J *et al* 2017 Design and modelling of a novel multilayered cylindrical magnetorheological brake *Int. J. Appl. Electromagn. Mech.* **53** 29–50
- [7] Shiao Y, Ngoc N A and Lai C 2016 Optimal design of a new multipole bilayer magnetorheological brake *Smart Mater. Struct.* **25** 115015
- [8] Gu T D and Maas J 2016 Long-term stable magnetorheological fluid brake for application in wind turbines *J. Intell. Mater. Syst. Struct.* **27** 2125–42
- [9] Wu J *et al* 2016 Design and modeling of a multi-pole and dual-gap magnetorheological brake with individual currents *Adv. Mech. Eng.* **8** 168781401665918
- [10] Song W *et al* 2017 Simulation and experimentation of a magnetorheological brake with adjustable gap *J. Intell. Mater. Syst. Struct.* **28** 1614–26
- [11] Rizzo R 2017 An innovative multi-gap clutch based on magneto-rheological fluids and electrodynamic effects: magnetic design and experimental characterization *Smart Mater. Struct.* **26** 015007
- [12] Bucchi F, Forte P and Frendo F 2015 Analysis of the torque characteristic of a magnetorheological clutch using neural networks *J. Intell. Mater. Syst. Struct.* **26** 680–9
- [13] Rizzo R *et al* 2015 A multi-gap magnetorheological clutch with permanent magnet *Smart Mater. Struct.* **24** 075012
- [14] Zheng J *et al* 2015 Transient multi-physics analysis of a magnetorheological shock absorber with the inverse Jiles–Atherton hysteresis model *Smart Mater. Struct.* **24** 105024
- [15] Nguyen T, Elahinia M and Wang S 2013 Hydraulic hybrid vehicle vibration isolation control with magnetorheological fluid mounts *Int. J. Veh. Des.* **63** 199
- [16] Barber D E and Carlson J D 2010 Performance characteristics of prototype MR engine mounts containing glycol MR fluids *J. Intell. Mater. Syst. Struct.* **21** 1509–16
- [17] Stoianovici D *et al* 2017 MR safe robot, FDA clearance, safety and feasibility of prostate biopsy clinical trial *IEEE/ASME Trans. Mechatronics* **22** 115–26
- [18] Lukianovich A *et al* 1996 Electrically controlled adjustable-resistance exercise equipment employing magnetorheological fluid 1996 *Symp. on Smart Structures and Materials* (International Society for Optics and Photonics)
- [19] Zhou W, Chew C and Hong G 2007 Development of a compact double-disk magneto-rheological fluid brake *Robotica* **25** 493–500
- [20] Sarkar C and Hirani H 2015 Development of a magnetorheological brake with a slotted disc *Proc. Inst. Mech. Eng. D* **229** 1907–24
- [21] Kikuchi T, Kobayashi K and Inoue A 2011 Gap-size effect of compact MR fluid brake *J. Intell. Mater. Syst. Struct.* **22** 1677–83
- [22] Senkal D and Gurocak H 2010 Serpentine flux path for high torque MRF brakes in haptics applications *Mechatronics* **20** 377–83
- [23] Rossa C *et al* 2014 Development of a multilayered wide-ranged torque magnetorheological brake *Smart Mater. Struct.* **23** 025028
- [24] Rossa C *et al* 2014 Design considerations for magnetorheological brakes *IEEE/ASME Trans. Mechatronics* **19** 1669–80
- [25] Shiao Y and Nguyen Q 2013 Development of a multi-pole magnetorheological brake *Smart Mater. Struct.* **22** 065008
- [26] Nguyen Q, Choi S and Wereley N M 2008 Optimal design of magnetorheological valves via a finite element method considering control energy and a time constant *Smart Mater. Struct.* **17** 025024
- [27] Lord Technical Data 2012 MRF-132DG magneto-rheological fluid www.lord.com
- [28] Tu F *et al* 2012 Experimental study and design on automobile suspension made of magneto-rheological damper *Energy Proc.* **16** 417–25
- [29] Liu B *et al* 2006 Development of an MR-brake-based haptic device *Smart Mater. Struct.* **15** 1960–6